THE JOURNAL OF BIOLOGICAL CHEMISTRY VOL. 286, NO. 31, pp. 27389–27398, August 5, 2011

Apolipoprotein L6, Induced in Atherosclerotic Lesions, Promotes Apoptosis and Blocks Beclin 1-dependent Autophagy in Atherosclerotic Cells*

Received for publication, December 7, 2010, and in revised form, May 29, 2011 Published, JBC Papers in Press, June 6, 2011, DOI 10.1074/jbc.M110.210245

Siqin Zhaorigetu[‡], Zhaoqing Yang[§], Ian Toma[§], Timothy A. McCaffrey[§], and Chien-An A. Hu[‡1]

From the [‡]Department of Biochemistry and Molecular Biology, University of New Mexico School of Medicine, Albuquerque, New Mexico 87131 and the [§]Department of Medicine, Division of Genomic Medicine, and The Richard B. and Lynne V. Cheney Cardiovascular Institute, The George Washington University, Washington, D. C. 20037

Inflammatory cytokine-regulated apoptosis and autophagy play pivotal roles in plaque rupture and thrombosis of atherosclerotic lesions. However, the molecular interplay between apoptosis and autophagy in vascular cells has not been investigated. Our prior study showed that human apolipoprotein L6 (ApoL6), a pro-apoptotic BH3-only member of the Bcl-2 family, was one of the downstream targets of interferon-γ (INFγ), which sensitizes atherosclerotic lesion-derived cells (LDCs) to Fas-induced apoptosis. To investigate whether ApoL6 plays a causal role in atherosclerotic apoptosis and autophagy, in this study, we demonstrate that IFNγ treatment itself strongly induces ApoL6, and ApoL6 is highly expressed and partially co-localized with activated caspase 3 in activated smooth muscle cells in atherosclerotic lesions. In addition, overexpression of ApoL6 promotes reactive oxygen species (ROS) generation, caspase activation, and subsequent apoptosis, which can be blocked by pan caspase inhibitor and ROS scavenger. Knockdown of ApoL6 expression by siApoL6 suppresses INFγ- and Fas-mediated apoptosis. Further, ApoL6 binds Bcl-X_L, one of the most abundant anti-death proteins in LDCs. Interestingly, forced ApoL6 expression in LDCs induces degradation of Beclin 1, accumulation of p62, and subsequent attenuation of LC3-II formation and translocation and thus autophagy, whereas siApoL6 treatment reverts the phenotype. Taken together, our results suggest that ApoL6 regulates both apoptosis and autophagy in SMCs. IFNγ-initiated, ApoL6-induced apoptosis in vascular cells may be an important factor causing plaque instability and a potential therapeutic target for treating atherosclerosis and cardiovascular disease.

Atherosclerosis, a chronic inflammatory disease and the principal cause of heart attack and stroke, contributes to at least 30% of all mortality in the United States (1, 2). The atherosclerotic lesion results from a dynamic interplay involving many elements of dysfunctional wound repair, including proliferation, matrix synthesis, autophagy (self-eating), and apoptosis, in response to insult of the vascular endothelial cells (ECs)[2] and smooth muscle cells (SMCs) of the artery wall (3, 4). The cross-talk between cytokines, chemokines, growth factors, oxidized lipid species/low density lipoproteins (LDLs), and reactive oxygen species (ROS) in atherosclerotic lesions determine cell survival and death (5, 6). Inflammation, based on the particular cellular context, can modulate proliferation or apoptosis (type I programmed cell death) of different cell-types, such as ECs, SMCs, and the inflammatory infiltrate (lymphocytes, and monocytes/macrophages) in atherosclerotic lesions (7, 8). With regard to cell death, it has been well documented that during the early stages of lesion development, apoptosis of macrophages contributes to the accumulation of extracellular LDLs and protein debris, while in the later stages, activated SMCs encapsulate the lipid-rich regions, and their persistence contributes to collagen synthesis, matrix accumulation and negative remodeling (9, 10). However, when apoptosis occurs in SMCs in the thin fibrous cap of advanced lesions, the plaque is prone to rupture, thereby triggering thrombosis and myocardial infarction. Thus, apoptosis is a major contributing factor to plaque instability and sudden coronary death (7, 8, 11, 12).

Autophagy, a cell survival mechanism, has been shown to induce type II programmed cell death (13, 14). Autophagy is an intracellular recycling process in which unwanted organelles and macromolecules are delivered and catabolized by lysosome-mediated degradation. Currently, there are 34 **au**toph**a**g**y** (Atg) genes identified as essential regulators and/or direct participants in autophagic pathways (13). For example, Beclin 1, or Atg 6/Vsp30, a regulatory component of the Class III PI3K complex, is essential for the initiation of autophagy. Overexpression of Beclin 1 induces autophagy, whereas down-regulation of Beclin 1 blocks autophagy (15). In addition, LC3, or Atg8, is also essential for the autophagy pathway: activation and translocation of lipidated LC3-II to autophagosomes is correlated with the induction of autophagy and is one of the markers of autophagy (13, 14). In vascular cells, it is believed that autophagy supports survival, and plays an important role in the

* This work was supported, in whole or in part, by National Institutes of Health Grants 3P20RR016480-04 (to C. A. A. H.) and AG12712 (to T. A. M.).

[1] To whom correspondence should be addressed: Department of Biochemistry and Molecular Biology, MSC08 4670, 1 University of New Mexico, Albuquerque, NM 87131-0001. Tel.: 505-272-8816; Fax: 505-272-6587; E-mail: AHu@salud.unm.edu.

[2] The abbreviations used are: ECs, endothelial cells; BH, Bcl-2 homology domain; DHE, dihydroethidium; DPI, diphenylene iodonium; HUVECs, human umbilical vein endothelial cells; IFN, interferon; LDCs, lesion-derived cells; MDC, monodansylcadaverine; ROS, reactive oxygen species; SMCs, smooth muscle cells; atg, autophagy; AD, adenovirus; AV, autophagic vesicle; MOMP, mitochondrial outer membrane permeabilization.

etiology of cardiomyopathy and atherosclerosis (3, 4, 16, 17). However, the molecular basis of autophagy in the pathogenesis of atherosclerosis remains poorly understood. The crosstalk between apoptosis and autophagy through specific regulators in SMCs may decide the overall fate of the cell.

It has been shown that increased apoptosis occurs in advanced human atherosclerotic lesions and is frequently associated with clinically unstable coronary artery lesions (6, 7). In general, apoptosis can be initiated extrinsically (through death receptors, *e.g.* Fas) or intrinsically (through mitochondria or endoplasmic reticulum stress), and all cell types present in atherosclerotic lesions can undergo apoptosis (18–20). Importantly, cells undergoing apoptosis need to be efficiently removed in atherosclerotic lesions. If not, rapid exposure of phosphatidylserine on the outer leaflet of the plasma membrane of apoptotic cells is a potent inducer of the generation of thrombin and activation of the coagulant cascade (21, 22). However, it has been shown that phagocytosis of apoptotic cells by lipid-loaded macrophages is severely impaired in advanced atherosclerotic lesions, resulting in accumulation of proinflammatory necrotic debris and plaque instability (23, 24). Moreover, the intracellular autophagy pathway in lipid-loaded macrophages has also been shown to be impaired (25). Thus, a better understanding of how apoptosis and autophagy are being regulated in vascular lesion cells is essential.

The Bcl-2 family members play critical roles in regulating and fine-tuning both apoptosis and autophagy, and their homeostatic balance determines cell fate (26–28). In a rabbit atherosclerotic model, increased levels of Bcl-X_L, an anti-apoptotic member of the Bcl-2 family, have been found in the intima of early proliferative lesions and the down-regulation of Bcl-X_L in neointima resulted in apoptosis of vascular cells and the regression of lesions (29). Likewise, higher Bcl-X_L levels were observed in apoptosis-resistant cells of human advanced lesions compared with control specimens, and had a protective effect against apoptotic insults (30). Moreover, our prior work in transcript profiling of lesion-derived cell (LDC) apoptosis revealed that up-regulated expression of Bcl-X_L is a major determinant of resistance to Fas-mediated apoptosis (31, 32). Subsequent investigation demonstrated that LDCs had elevated Bcl-X_L mRNA and protein that conferred resistance to Fas-induced apoptosis, which can be blocked by small molecule inhibitors or siRNA-knockdown of Bcl-X_L (32). Thus, Bcl-X_L is a potent apoptosis inhibitor in human LDCs. Moreover, recent evidence showed that apoptosis and autophagy are intimately interconnected, by sharing key molecular regulators, such as Bcl-2, Bcl-X_L, and Beclin 1 (33).

Utilizing microarray profiling, quantitative RT-PCR and immunoblot analysis, we recently showed that ApoL6, a BH3-only pro-apoptotic member of the Bcl-2 family, was one of the 36 major downstream targets of INFγ-sensitized, Fas-induced apoptosis in LDCs (34). These cell lines were originally isolated from the fibrous cap of human atherosclerotic lesions, possessing characteristics of myofibroblasts and were resistant to the antiproliferative effects of transforming growth factor-β and the pro-apoptotic effects of Fas ligation, similar to activated, apoptosis-resistant SMCs in neointima (35, 36). Although we documented that overexpression of ApoL6 induced mitochondria- and caspase 8-mediated apoptosis by release of apoptogenic factors from mitochondria and activation of caspases in various cells, including human umbilical vein endothelial cells (HUVECs) (37), the role of ApoL6 in atherosclerosis has not been explored. In this study, we investigated the link between ApoL6, ROS, Bcl-X_L, Beclin 1, and p62 in atherosclerotic plaque apoptosis and autophagy.

EXPERIMENTAL PROCEDURES

Cell Culture and Treatment—LDCs, with characteristics of SMC-like myofibroblasts, were established from the fibrous cap of human carotid artery atherosclerotic lesions as previously described (31, 36), and were cultured in M199 medium with Earle's buffered saline, L-glutamine, HEPES, 10% FBS, and gentamicin sulfate (50 μg/ml) (BioWhittaker). Prior microarray analysis indicates that LDCs express several consensus markers of SMC-like myofibroblasts including smooth muscle α-actin (ACTA2), smooth muscle myosin heavy chain (MYH11), calponin 1 (CNN1), aortic preferentially expressed protein 1 (APEG1), and SM22a/transgelin (TAGLN). LDCs were sensitized by IFNγ (10 nM; R&D Systems) to Fas-induced apoptosis as described (32).

Atherosclerotic Tissue Samples and Immunohistochemical Staining—Slides containing thin sections of paraffin-embedded human artery tissues with or without atherosclerotic lesions were obtained from carotid endarterectomy as waste surgical specimens under Institutional Review Board-approved protocols as previously described (31, 32, 35). Immunohistochemical staining was conducted as follow: slides were deparaffinized and then rehydrated. Antigen retrieval was performed by treating slides in citrate buffer (pH 6.0) in a microwave oven followed by blocking the endogenous peroxidase activity by incubating slides with 1% hydrogen peroxide for 30 min. Slides were then treated with 10% normal goat serum in 1x PBS at room temperature for 60 min to block nonspecific binding. Subsequently, slides were incubated with rabbit polyclonal anti-ApoL6 (1:100 dilution) (37) or anti-caspase 3 (9661; Cell Signaling, 1:200 dilution) at 4 °C for overnight, washed three times with 1× PBS, incubated with biotinylated goat anti-rabbit antibody at room temperature for 60 min, and then incubated with avidin-biotinylated peroxidase complex (Vectastain ABC Kit, Vector Laboratories) for 30 min followed by reacting with 3,3′-diaminobenzidine for color development. α-Actin, a marker for smooth muscle cells, was used as a control. Images were observed using a Zeiss A1 microscope with a digital camera (Optronics 60806).

ApoL6 Adenovirus (AD.ApoL6)—Construction of adenovirus (AD) harboring full-length ApoL6 cDNA (AD.ApoL6) and infection of cells by viruses were performed as previously described (37, 38). In one group, pan caspase inhibitor (Z-VAD-FMK, 50 μM; R&D Systems) was added 2 h prior and during viral infection for 48 h. Cell numbers and apoptosis were measured over time by cell counting, analysis of cell morphology, and assay of caspase activation as previously described (14, 37, 38).

Immunoblotting Assay—To prepare total cellular extracts, cells were isolated and sonicated in RIPA solution (0.01 M Tris-HCl, pH 8.0, 0.14 M NaCl, 1% sodium deoxycholate, 0.1% SDS,

and 1% Triton X-100). Protein concentrations were measured using the BCA protein assay reagent (Pierce). Proteins were separated using 10% SDS-PAGE (20–30 μg protein/lane) and transferred to nitrocellulose membranes (Bio-Rad) or polyvinyl difluoride (PVDF) (Pierce), which were then incubated with indicated antibodies, such as polyclonal anti-ApoL6, polyclonal anti-activated caspase 9 (9501S; Cell Signaling), monoclonal anti-activated caspase 8 (9746; Cell Signaling), polyclonal anti-activated caspase 3 (9661; Cell Signaling), polyclonal anti-protein A (P3775; Sigma), monoclonal anti-Bcl-X_L (2764; Cell Signaling), monoclonal α-tubulin (T9026, Sigma) and monoclonal anti-β-actin (AC-74; Sigma), anti-Beclin 1 (B6061; Sigma), and anti-p62 (610832; BD Transduction Laboratory). Subsequently, blots were incubated with goat anti-rabbit or anti-mouse HRP-labeled secondary antibodies, as previously described (37).

Construction and Expression of pApoL6-EGFP—The full-length cDNA of ApoL6 (37) was subcloned into the XhoI (5′) and EcoR I (3′) sites of pEGFP-N1 (Clontech). The in-frame fusion construct, pApoL6-EGFP, was confirmed by sequencing. Transient co-transfection of LDCs was carried out using a 1:1 mixture of pApoL6-EGFP and pmcherry-LC3 (39) with Lipofectamine 2000 reagent (Invitrogen). 24 h after co-transfection, cells were incubated in HBSS, an isotonic buffer lacking nutrients, for 2 h to induce autophagy, and then subjected to confocal microscopy analysis as previously described (38).

siApoL6, IFN-γ, and Anti-Fas Treatment in LDC Cells—siRNA treatment: Both siControl (cyclophilin B) and OnTarget siApoL6 Smart Pool, containing 4 target sequences, were purchased from Dharmacon. Cells were seeded in 24-well plate (50,000 cells/well). The transfection was performed the next day after seeding in 2% FBS media with siControl or siApoL6 diluted in antibiotic-free medium using the DharmaFECT transfection reagent. siRNA was added to respective wells to a final dose of 10 nM. Media were changed the next day after siRNA transfection, and cells allowed to recover. The next morning, cells were treated with recombinant human IFNγ (R&D Systems, 5 ng/50 IU/ml) in 1% FBS media, and 8 h later the sensitivity to apoptosis was examined by determining survival after challenge with a Fas-activating IgM (clone CH11; Upstate Biotechnology) (10 or 25 ng/ml). 20 h later, MTT was added for 4 h, the stained cells were dissolved in DMSO, and the level of reduced MTT was measured by absorbance at 540 nm in a plate reader (34). The efficiency of target silencing was assessed by quantitative RT-PCR (qPCR) mRNA expression level and/or Western blot analysis with anti-ApoL6 antibody.

ROS Detection and Autophagy Flux Determination by Fluorescence Microscopy—LDCs were grown on glass coverslips, treated as indicated, fixed in 4% (v/v) PBS-buffered paraformaldehyde solution and subjected to fluorescent microscopic analysis as described (14, 38). Two methods were used to assay ROS generation in cells using the fluorescence dye DHE (dihydroethidium; Sigma) (38, 40). In brief, LDCs were plated on a glass slip in 6-well plates in medium, infected with indicated virus (AD or AD.ApoL6), with or without 1 μM DPI (diphenylene iodonium; Sigma). After infection for 24 and 30 h, DHE was added to the cell culture (final concentration 2 μM), incubated for an additional 30 min, and washed twice with PBS. For image analysis, fixed cells on coverslips were mounted on glass slides and observed under a fluorescence microscope. For fluorescence quantitative analysis, cells were trypsinized from coverslips, resuspended in ice-cold PBS, fixed and then analyzed using a FACScan flow cytometer (Beckon Dickinson; excitation 248 nm, emission 585 nm) as described (38). To monitor blockage of autophagy flux, LDCs were infected with AD or AD.ApoL6 for 24, 36, and 48 h, stained with monodansylcadaverine (MDC; 50 μM) for 1 h at 37 °C, washed four times with PBS, and followed by fixation with 4% paraformaldehyde for 15 min at room temperature. Cell images were taken and acidic autophagic vesicles/compartments labeled with MDC in cells were counted by a Zeiss AxioScope A1 epifluorescence microscope (Carl Zeiss MicroImaging, Inc.).

Immunoprecipitation Using Anti-ApoL6 Antibody and Protein A-Agarose Beads—To identify ApoL6-binding protein(s), LDC.2 cells were infected with AD or AD.ApoL6 for 30 h and then total protein extracts were prepared. For sample pre-clearing, protein extracts were first incubated with 50 μl of protein A-agarose beads (sc-2001; Santa Cruz Biotechnology) on ice for 1 h. Anti-ApoL6 antibody was then added to the pre-treated and incubated at 4 °C overnight. 50 μl of protein A beads were added to the mixture and incubated for 2 h at 4 °C. Subsequently, beads were washed 10 times in cold RIPA buffer and resuspended in 2× SDS-PAGE sample buffer. Equal amounts (20 μg) of protein samples from the eluted and unbound/wash-through were separated by SDS-PAGE followed by immunoblot analysis.

Transmission Electron Microscopy (TEM) Analysis—LDCs cultured on coverslips were infected with AD or AD.ApoL6 for 30 h, fixed, embedded, and then ultra-thin sectioned for TEM analysis. Images were examined, captured and processed using an Hitachi H-7500 EM, AMT XR60B camera and associated software (v.5.42) as previously described (14, 41, 42). To count autophagic vesicles (AVs) in cells, we defined AVs as double-membrane structures greater than 1 μM in size. High-magnification pictures of TEM images were used to count and calculate AVs per cross-sectioned cell by two independent investigators. At least 200 cells were counted from each group.

Statistical Analysis—Triple biological and experimental replicates were used for statistical analysis. Data are expressed as mean ± S.E. Comparison between experimental groups was made using Student's *t* test. A *p* value of less than 0.05 was considered statistically significant.

RESULTS

ApoL6 Expression Is Inducible by IFNγ in LDCs and HUVECs—In a systematic identification of candidate genes important in IFNγ sensitized, Fas-induced apoptosis in LDCs, our prior study suggested that ApoL6 was one of the up-regulated, downstream effectors of IFNγ in LDCs apoptosis (26). To confirm and extend this observation at the protein level and other cell-types, two LDC lines, LDC.1 and LDC.2, and HUVECs, a widely used model for endothelial cells, were treated with IFNγ. Immunoblot analysis showed that ApoL6 expression was significantly induced by IFNγ in both LDC lines and HUVECs, implying that ApoL6 has the same interferon responsiveness in both cell types (Fig. 1). Importantly, endogenous expression of

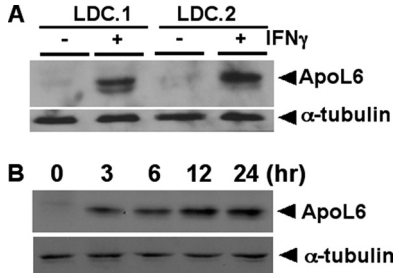

FIGURE 1. **ApoL6 expression is inducible by IFNγ in LDCs and HUVECs.** *A*, two LDC cell lines, LDC.1 and LDC.2 and *B*, HUVECs were treated with IFNγ for 6 h and the indicated times, respectively. Total soluble protein extracts were used for immunoblot analysis and then probed with anti-ApoL6 and α-tubulin antibodies. Expression of ApoL6 was significantly up-regulated by IFNγ in both LDCs and HUVECs.

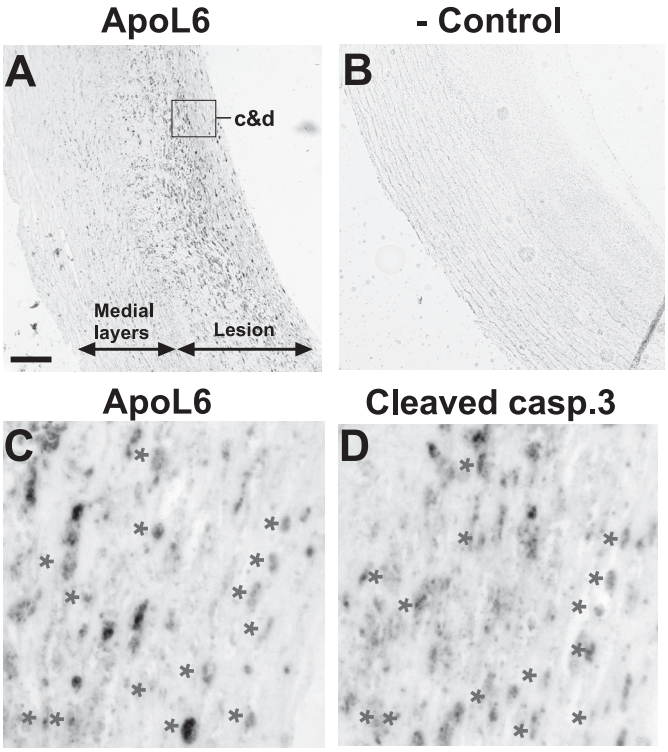

FIGURE 2. **ApoL6 is highly expressed in and partially co-localized with activated caspase 3 in SMCs within atherosclerotic lesions.** Immunohistochemical staining of adjacent sections using anti-ApoL6 (*A* and *C*) and anti-cleaved/activated caspase 3 antibody (*D*). Both antibodies showed intense, specific staining in activated SMCs in the neointima of the lesions. SMCs double positive of ApoL6 and activated caspase 3 (indicated by *) were ApoL6-positive cells undergoing caspase 3 dependent apoptosis. *B* was a negative control without probing with a primary antibody.

ApoL6 was very basal in HUVECs and inducible by IFNγ 3 h after treatment (Fig. 1*B*).

ApoL6 Is Significantly Overexpressed in Activated Smooth Muscle Cells and Partially Co-localized with Cleaved Caspase 3 in Atherosclerotic Lesions of Carotid Artery—Immunohistochemical staining of adjacent slides using anti-ApoL6 (Fig. 2, *panel a*), negative control antibody (*panel b*), and anti-cleaved/activated caspase 3 antibody (*panel d*). *Panels c* and *d* were the 20× magnified images of the boxed area of *panel a*. Both antibodies showed intense, specific staining of activated SMCs in the neointima of the lesions, with weaker staining in the superficial layers of the tunica media. SMCs double positive of ApoL6 and activated caspase 3 (indicated by *) were ApoL6-positive cells undergoing caspase 3-dependent apoptosis. The staining of ApoL6 or cleaved caspase 3 (cells in dark) was consistent with staining with anti-α-actin (data not shown).

ApoL6-induced ROS Generation and Subsequent Apoptosis in LDCs—Previously, we showed that overexpression of ApoL6 induced caspase 8- and mitochondria-mediated apoptosis in various cell-types, including HUVECs (37). To further investigate the function of ApoL6 in LDCs, we used adenovirus harboring wild-type full-length ApoL6 (AD.ApoL6) and AD only to infect LDCs. As shown in Fig. 3*A*, AD.ApoL6 was able to induce apoptosis in LDCs, both LDC.1 and LDC.2, 30 h after infection (*panels c* and *d*). Cells infected with AD.ApoL6 showed fewer attached cells with a change in morphology (rounded and condensed; see cells labeled with triangles). In addition, we showed a time-dependent induction of apoptosis by ApoL6 in LDCs infected with AD.ApoL6 (Fig. 3*B*, *columns 6–9*) compared with that of AD (Fig. 3*B*, *columns 1–4*). Pan caspase inhibitor, Z-VAD-FMK, partially blocked ApoL6-induced apoptosis (Fig. 3*B*, *column 10*), but had no cytotoxic effect on LDCs infected with AD control (Fig. 3*B*, *column 5*). Thus, we confirmed that ApoL6 functioned as an apoptosis inducer in LDCs, as in other cell-types previously described (29). To explore the link between ROS and ApoL6 in LDC apoptosis, we investigated whether ApoL6 overexpression caused ROS generation in LDCs. As shown in Figs. 3*C*, *panel e* and *2nd column* in 3*D*, greater amounts of ROS were generated in LDCs infected with AD.ApoL6 30 h after induction as compared with control (AD; Fig. 3*C*, *panel b* and *column 1* in 3*D*).

Antioxidant DPI Partially Blunts ApoL6-induced Apoptosis and ROS Generation in LDC Cells—It is well documented that increased amounts of ROS induce apoptosis in human cells, and our prior studies showed that DPI, a ROS inhibitor and a potent antioxidant, strongly inhibited POX-, PUMA-, and p53-induced apoptosis (38, 40). To determine if ApoL6-induced apoptosis was related to increased ROS generation, the effect of DPI on cell survival was tested. We first conducted a cytotoxicity experiment and found that 1 μM of DPI was not toxic to LDCs (<5% of cell death), but somehow altered cell morphology (Fig. 3*C*, *panels c* and *f*). Subsequently, a test was conducted to determine the ability of DPI to protect AD.ApoL6-infected LDCs. Our results showed that 1 μM of DPI reduced ROS generation (Fig. 3*C*, *panels f* and *3rd column* in Fig. 3*D*), and protected LDC cells from death when infected with AD.ApoL6 (Fig. 3*E*). Quantification of ROS generation by flow cytometric analysis showed that there was a 2.2-fold increase of ROS in LDCs infected with AD.ApoL6 as compared with that of AD, and DPI significantly blocked the generation of ROS in LDCs cells infected with AD.ApoL6 (Fig. 3*D*). Notably, neither AD nor DPI alone induced apoptosis in LDCs (Fig. 3*E*). These results were consistent with the finding that DPI blocks POX- or PUMA-induced ROS generation and apoptosis in mammalian cells (38, 40). Thus, ApoL6-induced apoptosis in LDCs is, in part, through the oxidative stress mechanism.

siRNA Knockdown of ApoL6 Partially Rescues IFNγ-initiated, Fas-mediated Apoptosis in LDCs—To address whether ApoL6 is a causal factor in IFNγ and Fas-mediated apoptosis in LDCs, we utilized siApoL6 and three different concentrations of anti-Fas IgM in IFNγ-sensitized LDCs. As shown in Fig. 3*F*, immu-

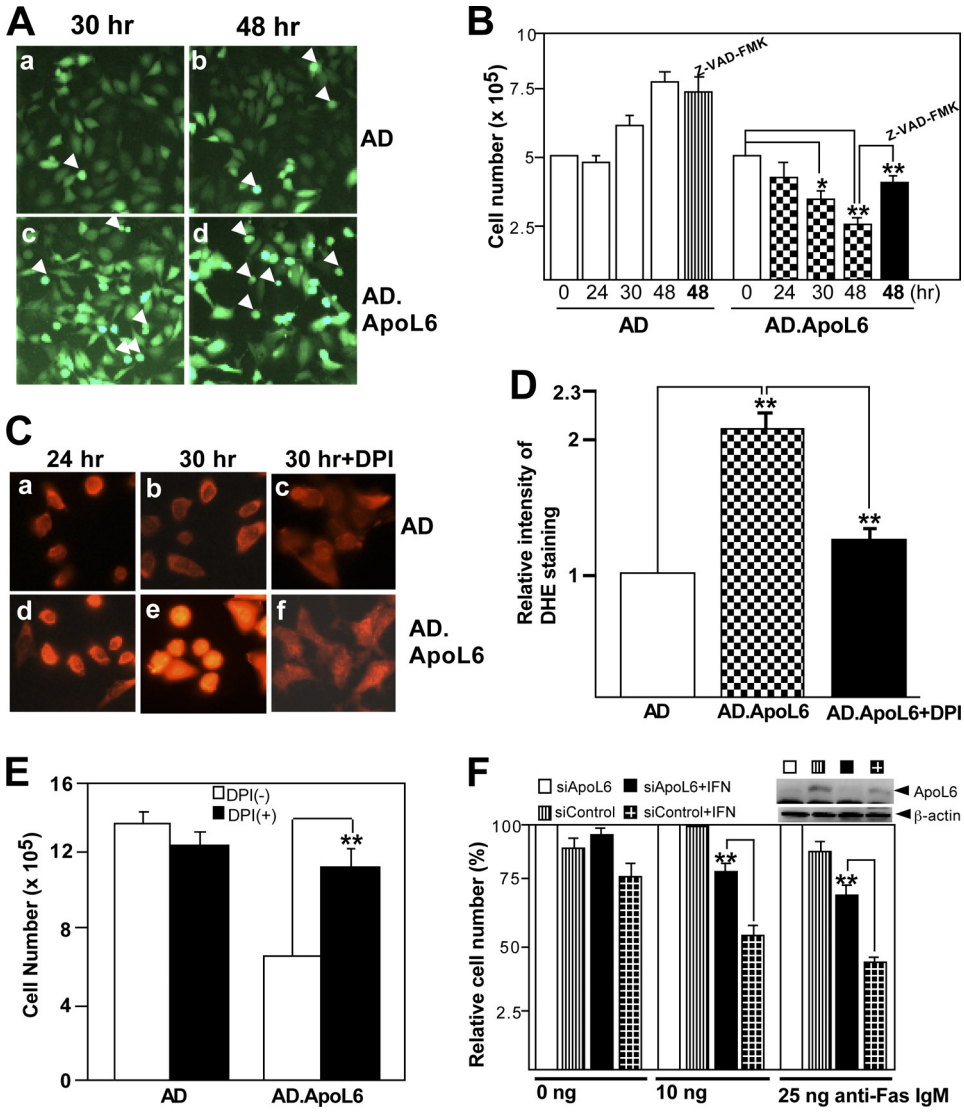

FIGURE 3. **ApoL6 induces cell death, in part, through ROS generation, which can be blunted by z-VAD-fmc, antioxidant DPI, and siApoL6 treatment.** *A* and *B*, time-dependent induction of apoptosis by ApoL6 in LDCs. LDCs cells were infected with adenovirus only (*AD*) or AD harboring wild-type full-length ApoL6 cDNA (AD.ApoL6). AD.ApoL6 infected cells showed profound apoptosis 48 h after infection, as indicated by increased accumulation of dead cells (labeled with *triangles* in *A*) and fewer attached cells (8th and 9th columns of *B*). ApoL6-induced cell death in LDCs was partially blunted by pan caspase inhibitor, Z-VAD-FMK (10th column of *B*). Z-VAD-FMK has no cytotoxic effect on LDCs infected by AD control (5th column of *B*). Cells that were infected with AD or AD.ApoL6 were in green because both viruses carried EGFP gene as a marker. *C*, ApoL6 induces ROS generation in LDC cells, which is blunted by DPI. Cells were infected with AD or AD.ApoL6 for 24 and 30 h and then incubated with the fluorescent, ROS/superoxide-sensitive dye DHE with or without DPI (1 μM). ROS generation was observed under a fluorescence microscope. Greater amounts of ROS were generated in LDCs cells infected with AD.ApoL6 (*panels d* and *e*), as compared with AD control (*panels a* and *b*). In addition, DPI significantly blocked the generation of ROS in LDCs cells infected with AD.ApoL6 (*panel f* and 3rd column in *D*). *D*, quantification of ROS by flow cytometric measurements. Intensities of DHE fluorescence in *C* with or without DPI were measured by a flow cytometer. There was a 2.2-fold increase of ROS in LDCs infected with AD.ApoL6 (*2nd column*) as compared with that of AD (*1st column*), while DPI reduced ROS production in cells infected with AD.ApoL6 (*3rd column*). The value for the cells infected with AD only was set to be 1, and the other values were normalized to AD only. *E*, DPI-protected cells from apoptosis. Cells were infected with AD or AD.ApoL6 in the presence or absence of DPI for 30 h and then cell numbers were counted. As shown in *panel C*(*f*) and in the *4th column* of *E*, DPI blocked apoptosis in LDCs cells infected with AD.ApoL6. Note that DPI altered the cell morphology but had no cytotoxicity effect on LDCs in this concentration. *F*, siApoL6 treatment blunted IFNγ-initiated and Fas-mediated apoptosis in LDCs. MTT assay indicated that siRNA knockdown of ApoL6 reduced IFNγ-treated and Fas-mediated apoptosis in LDCs. Neither IFNγ nor anti-Fas IgM alone in the presence or absence of siApoL6 induced cell death. All the EGFP and DHE staining images of *A* and *C* were taken by the same microscope (Zeiss A1) with the CCD camera (Optronics), and the same parameters (*e.g.* exposure time, 4 ms). Bars represent mean $\pm$ S.E. ($n = 4$, *, $p < 0.05$; **, $p < 0.01$, significant difference comparing to the indicated sample by Student's *t* test).

noblot analysis demonstrated that siApoL6 greatly reduced the levels of ApoL6 expression in both IFNγ-treated or -untreated cells. Cells without IFNγ treatment were alive after 24 h treatment with 0, 10, and 25 ng/ml of anti-Fas IgM in the presence or absence of siApoL6 (*columns 1*, *2*, *5*, *6*, *9*, and *10*). However, when cells were treated with 5 ng/ml of IFNγ, there was a concentration-dependent apoptosis in LDCs in the presence of anti-Fas IgM (*columns 4*, *8*, and *12*). Importantly, siApoL6 significantly blocked the apoptosis in LDCs treated with 10 ng or 25 ng anti-Fas IgM (*columns 7* and *11*).

ApoL6 Interacts with Bcl-X_L in LDCs—The BH3-only proteins, of which ApoL6 is one, are pro-death regulators in apoptosis through interaction with anti-death members of the Bcl-2 family members, such as Bcl-2, Bcl-X_L, and Mcl-1 (19, 27,

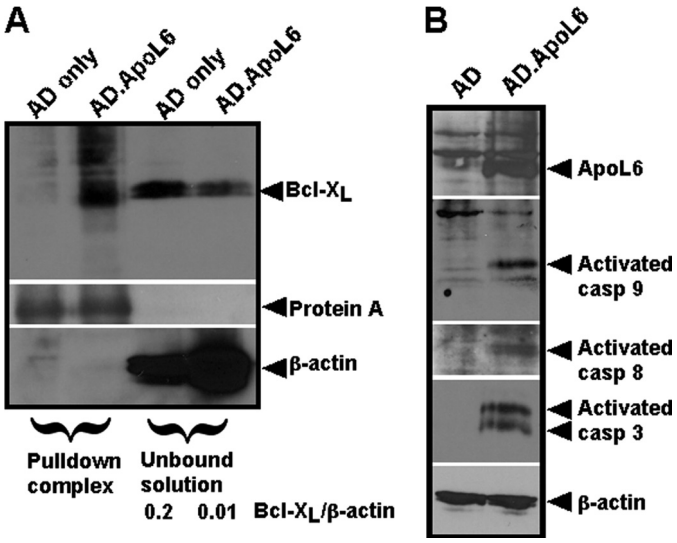

FIGURE 4. **ApoL6 interacts with Bcl-X_L and induces activation of caspases 9, 8, and 3 in LDCs.** *A,* immunoprecipitation and immunoblot analysis revealed that ApoL6 interacted with Bcl-X_L. LDCs cells were infected with AD only (*lane 1*) or AD.ApoL6 (*lane 2*) and total soluble protein extracts from infected cells were used for immunoprecipitation by anti-ApoL6 and then protein A beads. A 30 kDa band corresponding to Bcl-X_L co-immunoprecipitated with ApoL6 from LDCs cells infected with AD.ApoL6 (*lane 2*), but not from cells infected with AD (*lane 1*). *Lanes 3* and *4*, the unbound protein solutions after immunoprecipitation from cells infected with AD and AD.ApoL6, respectively. As shown, the endogenous expression of Bcl-X_L was abundant in LDCs cells infected with AD or AD.ApoL6. However, shown in *lane 1*, without AD.ApoL6 infection, Bcl-X_L was not co-immunoprecipitated by anti-ApoL6 and protein A beads. Protein A was used as loading control for the pulldown complexes, while β-actin was used as loading control for the unbound solutions. The ratios between Bcl-X_L and β-actin in the unbound solutions were indicated. *B,* WB analysis showed that the endogenous expression of ApoL6 in LDCs cells infected with AD for 30 h was very low, which was consistent with the finding in LDC cells without IFNγ treatment (see Fig. 1). In contrast, LDCs cells infected with AD.ApoL6 (30 h) showed an increased expression of ApoL6 (*top panel*). Overexpression of ApoL6 induced cleavage and activation of pro-caspases 9, 8, and 3 to their corresponding active forms (caspase 9, 37 kDa; caspase 8, 43, and 41 kDa; and caspase 3, 19, and 17 kDa). β-actin was used as a loading control.

28, 43). To investigate whether ApoL6 physically interacted with cell death regulators, we conducted immunoprecipitation and immunoblot analysis of ApoL6-containing complexes isolated from LDCs infected with AD.ApoL6. We observed a band of ~30 kDa corresponding to Bcl-X_L present in the pulldown complexes of ApoL6 by anti-ApoL6 and then protein A beads from cells infected with AD.ApoL6 (Fig. 4*A*, *lane 2*), but not from cells infected with AD only (Fig. 4*A*, *lane 1*), demonstrating that ApoL6 interacted with Bcl-X_L. As revealed in the unbound solutions (Fig. 4*A*, *lanes 3* and *4*), endogenous expression of Bcl-X_L was abundant in LDCs infected with AD or AD.ApoL6, but because ApoL6 bound Bcl-X_L (*lane 2*), the intensity of the Bcl-X_L band was greatly reduced in lane 4 when normalized with β-actin. Moreover, in the same pulldown experiment, we did not find ApoL6 physically interacted with Bcl-2 or Mcl-1 (data not shown). Importantly, we have previously documented that LDCs possessed elevated Bcl-X_L mRNA and protein levels that inhibited caspase activation and apoptosis (34). Thus, the binding and sequestration of Bcl-X_L by ApoL6 would contribute to LDCs vulnerability to apoptosis under inflammatory conditions.

ApoL6 Induces Activation of Caspases 9, 3, and 8—Activation of caspase(s) is a hallmark of apoptosis (19, 37, 43). We investigated whether overexpression of ApoL6 induced activation of caspase 9 (37 kDa), caspase 8 (43/41 kDa), and caspase 3 (19/17 kDa) in LDCs using immunoblot analysis. Fig. 4*B* showed that LDCs cells infected with AD.ApoL6 after 30 h produced a significant amount of ApoL6, and overexpression of ApoL6 induced cleavage and activation of pro-caspases 9, 8, and 3 to their corresponding active forms. Thus, activation of caspases, together with ROS toxicity, led to profound apoptotic cell death. In contrast, control AD did not induce caspase activation in LDC.2 cells.

ApoL6 Affects Beclin 1, p62, LC3, and Autophagy, which Can Be Reversed by siApoL6 Treatment—To investigate the role of ApoL6 in autophagy, we measured the effect of ApoL6 on four autophagy markers, 1) Beclin 1/Atg6/Vps30, an autophagy essential protein (15, 43, 44); 2) P62 (also known as SQSTM1/sequestome 1), an adaptor protein targeting protein aggregates and damaged organelles for autophagic degradation (39, 43–45). In so functioning, p62 is selectively incorporated into autophagosomes through binding to LC3-II, degraded by autophagy (46) and a good marker for efficient autophagic activity; 3) LC3/Atg8, activation and translocation during autophagy (14, 39, 43, 44); and 4) Autophagic vesicles (AVs)/compartments: autophagosomes, amphisomes and autolysosomes (13, 43, 44). First, using LDCs infected with AD.ApoL6 and immunoblot analysis, we showed time-dependent Beclin 1 degradation 24 h after infection, whereas p62 was increased reciprocally (Fig. 5, *A* and *B*). Second, we observed that starvation treatment of LDCs infected with AD only in HBSS induced LC3-II activation (Fig. 5*C*, *lane 4*), demonstrating induction of autophagy, whereas LDCs infected with AD.ApoL6 blocked LC3-II activation under starvation condition (Fig. 5*C*, *lane 5*). Third, to further demonstrate that ApoL6 overexpression inhibited autophagy in normal and starvation-induced autophagy conditions, we co-transfected LDCs with pApoL6-EGFP and pmcherry-LC3 and then treated the cells with starvation medium. We first confirmed that forced transient expression of pApoL6-EGFP in LDCs also induced apoptosis, same as the effect of AD-ApoL6 (data not shown). We then showed that cells co-transfected with pEGFP-N1 (control plasmid) and pmcherry-LC3 in regular medium exhibited co-localized, cytosolic patterning of green (EGFP, Fig. 6, *panel a*) and cherry (cherry-LC3, *panel b*), and when merged, appeared yellow (*panel c*). When these cells were incubated in starvation medium, increased punctate structures (in cherry) were observed, indicating the formation of AVs (*panels e* and *f*). However, the EGFP remained cytosolic (*panel d*). Importantly, when cells were co-transfected with pApoL6-EGFP and pmcherry-LC3 incubated in control medium, both ApoL6-EGFP protein (in *green*) and cherry-LC3 (*cherry*) were predominantly cytosolic (*panels g* and *h*) with some ApoL6-EGFP localized in granular/punctate structures (*panels g* and *i*). However, when these cells were incubated in starvation medium, both ApoL6-EGFP and cherry-LC3 remained cytosolic (*panels j* and *k*) with almost no cherry puncta detected in the cytosol (*panels k* and *l*). This demonstrated that ApoL6-EGFP inhibited the translocation of Cherry-LC3 to AVs, and therefore autophagy, during the induction of apoptosis. Conversely, when ApoL6 expression was knocked down by siApoL6 in IFNγ-treated

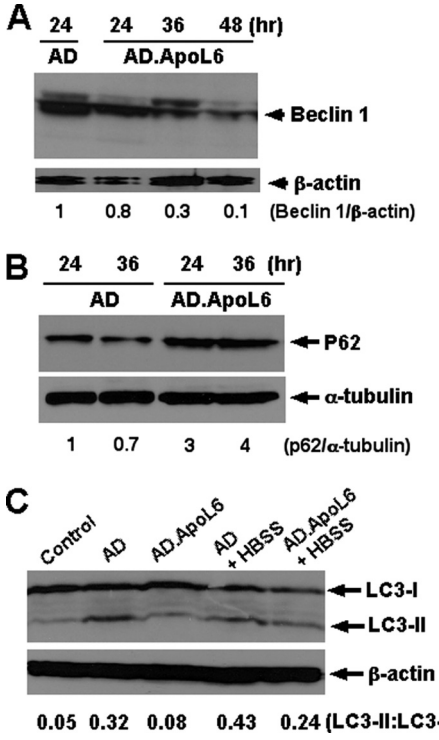

FIGURE 5. **Overexpression of ApoL6 induces Beclin 1 degradation and p62 accumulation, and inhibits LC3-II activation in LDCs.** *A*, Beclin 1 showed time-dependent decrease after AD.ApoL6 infection, *B*, P62 showed time-dependent increase, and *C*, LC3-II activation was blocked in both regular and starvation (HBSS)-stressed autophagic conditions in LDCs infected with AD.ApoL6. The ratios of indicated protein bands are shown numerically *below* each panel.

LDCs, expression of Beclin 1 and LC3-II were up-regulated whereas expression of p62 was down-regulated (Fig. 6*B*). Fourth, to further analyze AV formation, LDCs infected with AD.ApoL6 or AD control were subjected to TEM analysis and AV count. We defined AVs as double-membraned structures, size greater than 1 μm (Fig. 7*A*, *panel c* as an illustration) (41, 42, 44). After counting and analysis, we showed that LDCs infected with AD.ApoL6 for 36 h had fewer AVs (~0.5 AV/cell; *panels b* and *d*) as compared with the control (~1.5 AV/cell; *panels a* and *d*). LDCs infected with AD control showed more large vacuoles and AVs (*panel a* as an illustration) whereas LDCs infected with AD-ApoL6 possessed fewer large vacuoles and AVs (*panel b* as an illustration). In addition, infected LDCs were stained with MDC, a fluorescence dye that recognizes acidic AVs (44, 47). LDCs infected with AD.ApoL6 showed significant reduction in numbers of acidic AVs per cell (to ~25%; Fig. 7*B*, *panel b* and *column 2 in panel C*), as compared with LDCs infected with AD only (Fig. 7*B, panel a* and *column 1* in *panel C*). These results were consistent with those of TEM analysis. Taken all together, our results clearly demonstrated that ApoL6 inhibited Beclin 1- and LC3-dependent autophagy.

DISCUSSION

Apoptosis has been closely associated with atherosclerosis because a higher apoptotic index has been observed in advanced atherosclerotic lesions compared with early ones (29, 30, 48). In the later stages of atherogenesis, up-regulated apoptosis in combination with impaired, cytoprotective autophagy in SMCs within the thin fibrous cap of lesions can promote plaque rupture, thrombosis, and subsequent myocardial infarction and stroke (1, 3, 4). Moreover, it has been shown that all major coronary arteries that undergo atherosclerosis usually display multiple vulnerable plaques in unstable patients (48). Thus, a favorable therapeutic strategy would be to simultaneously target inhibition of apoptosis and promotion of autophagy in activated SMCs to favor SMC survival and subsequent plaque stabilization. Our results in this study suggest that ApoL6 is a promising target for this purpose because ApoL6 plays an important role in regulating both apoptosis and autophagy in SMCs. First, utilizing human atherosclerotic lesion and normal tissue samples, we showed that expression of ApoL6, a downstream effector of IFNγ and *bona fide* BH3-only pro-death regulator, was up-regulated and partially colocalized with activated caspase 3 in SMCs in the neointima layer of atherosclerotic lesions (Fig. 2). In addition, we demonstrated that ApoL6 bound to Bcl-X_L, induced strong ROS generation, caspase activation, and subsequent apoptosis in LDCs (Figs. 3 and 4), and ROS scavenger and caspase inhibitor independently blocked ApoL6-induced apoptosis. Moreover, siApoL6 partially blunted caspase 3 activation and IFNγ-initiated and Fas ligation-mediated apoptosis (Figs. 3*F* and 6*B*). Taken together, the SMCs in lesion plaques that were double positive for ApoL6 and activated caspase 3 were also apoptotic, suggesting a causal role of ApoL6-induced apoptosis in vascular cells *in vivo*.

Importantly, five lines of evidence suggested that ApoL6 blocked autophagy. First, ApoL6 induced time-dependent degradation of Beclin 1/Atg6, an essential autophagy protein (Fig. 5*A*). Second, ApoL6 caused p62 accumulation reciprocal to Beclin 1 degradation (Fig. 5*B*). P62, an abundantly expressed signaling adaptor protein, is important for homeostatic and cytoprotective degradation of protein/organelle aggregates (45). It has been shown that p62 regulates the packing and delivery of polyubiquitinated, misfolded protein aggregates and dysfunctional organelles for autophagy-mediated clearance in mammalian cells (46). In fact, p62 is selectively engulfed into autophagosomes through direct binding to LC3-II and is degraded by autophagy (49, 50). Thus, the total levels of p62 inversely correlate with Beclin 1- and LC3-II-dependent autophagic activity. Third, forced transient expression of ApoL6 by AD.ApoL6 virus or pApoL6-EGFP plasmid in LDCs inhibited LC3-II activation and translocation in both regular and starvation conditions (Figs. 5*C* and 6*A*). In fact, atherosclerotic lesion cells *in vivo* are subjected to starvation stress due to hypoxia and inflammation conditions (1, 4, 23). Fourth, both electron and fluorescence microscopy analysis showed that ApoL6 blocked autophagy flux by decreasing the formation of autophagic vesicles/compartments (Fig. 7). Fifth, down-regulation of ApoL6 by siApoL6 in IFNγ-treated cells demonstrated a reversed autophagy phenotype, that is, increased expression of Beclin 1 and LC3 II and decreased expression of p62, as compared with ApoL6-overexpressing cells (Fig. 6*B*). Thus, not only did ApoL6 induce apoptosis, but also blocked Beclin 1-dependent cytoprotective autophagy. To our knowledge, ApoL6 is the first BH3-only protein that, when up-regulated, simultaneously promotes apoptosis and blocks autophagy, and is an attractive marker and target for treating atherosclerosis.

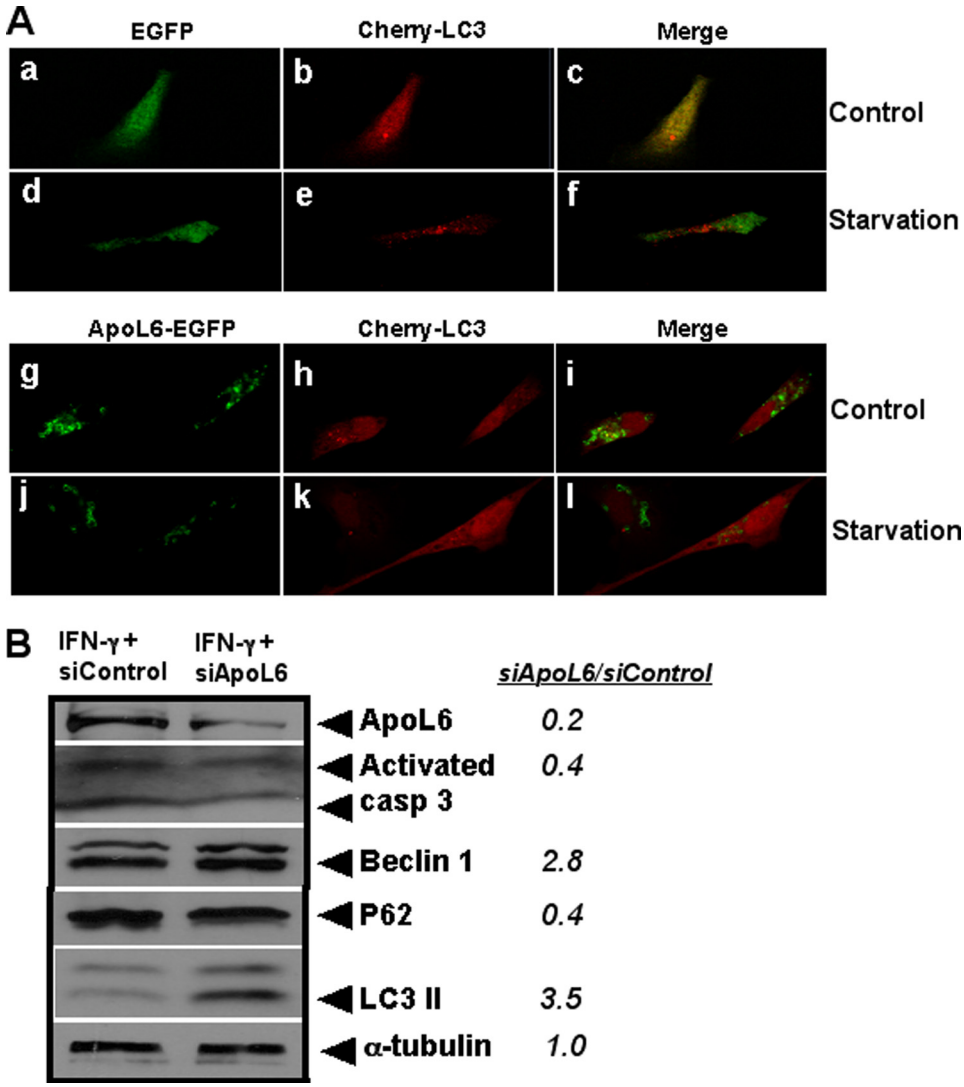

FIGURE 6. *A*, ApoL6 inhibits starvation induced LC3-II translocation and autophagy. Confocal microscopy analysis showed that LDCs co-transfected with pEGFP-N1 (control plasmid) and pmcherry-LC3 in control medium exhibited co-localized, cytosolic patterning of green (EGFP, *panel a*) and cherry (cherry-LC3, *panel b*), and when merged, appeared yellow (*panel c*). When these cells were incubated in starvation medium (HBSS), increased punctate structures in cherry were observed, indicating the formation of autophagic vesicles (*panels e* and *f*). However, the EGFP protein remained cytosolic (*panel d*). When LDcs were co-transfected with pApoL6-EGFP and pmcherry-LC3 in control medium, both ApoL6-EGFP fusion protein (*panel g*, in *green*) and cherry-LC3 (*panel h* in *cherry*) were predominantly cytosolic with some ApoL6-EGFP localized in punctate structures (*panels g* and *i*). However, when these cells were incubated in starvation medium, both ApoL6-EGFP and cherry-LC3 remained cytosolic (*panels j* and *k*) with almost no cherry puncta detected in the cytosol (*panels k* and *l*). *B*, LDCs were treated with IFNγ in the presence and absence of siApoL6 for 36 h. SiApoL6 treatment down-regulated ApoL6, caspase 3 activation and p62, while up-regulated Beclin 1 and LC3-II. The ratios of indicated protein bands between siApoL6/siControls are also indicated.

We and others (31, 32, 51, 52) have shown that IFNγ could sensitize Fas-induced SMC apoptosis, which is Bcl-X_L reversible. Bcl-X_L, a well-known anti-apoptotic factor, is up-regulated in apoptosis-resistant vascular cells. In this study, we showed that ApoL6 was able to sequester Bcl-X_L, promote ROS generation, induce caspase activation and apoptosis in LDCs (Figs. 3 and 4). It has been shown that BH3-only proteins, for example, PUMA, Noxa and Bad, after induction or post-translational activation, inactivate the anti-apoptotic Bcl-2 family members, such as Bcl-X_L, Bcl-2, and Mcl-1 (28). This relieves inhibition of Bax and Bak oligomerization/activation on the mitochondria outer membrane, which in turn promotes apoptosis. Once activated and liberated, Bax and/or Bak induces mitochondrial outer membrane permeabilization (MOMP) and subsequent release of apoptogenic factors for the activation of caspases. In addition, MOMP also results secondarily in elaboration of ROS, causing peroxidation of macromolecules, damage of membranes, deterioration of organelles, such as the ER and lysosomes, which impair normal cellular homeostasis leading to cell death (43). It is well known that ROS play important roles throughout atherogenesis. In early atherosclerosis, ROS stimulate SMC growth, whereas in late stages of lesion development, ROS induce SMC apoptosis, causing plaque instability (6, 7, 11). We concluded, therefore, that the generation of ROS and oxidative stress were also involved in ApoL6-induced apoptosis in LDCs (Fig. 8).

Interestingly, recent studies showed that apoptosis blocked Beclin 1-dependent autophagosome synthesis and subsequent autophagy: an effect rescued by Bcl-X_L in HeLa cells (53–54). In addition, Hou and colleagues showed that cytoprotective

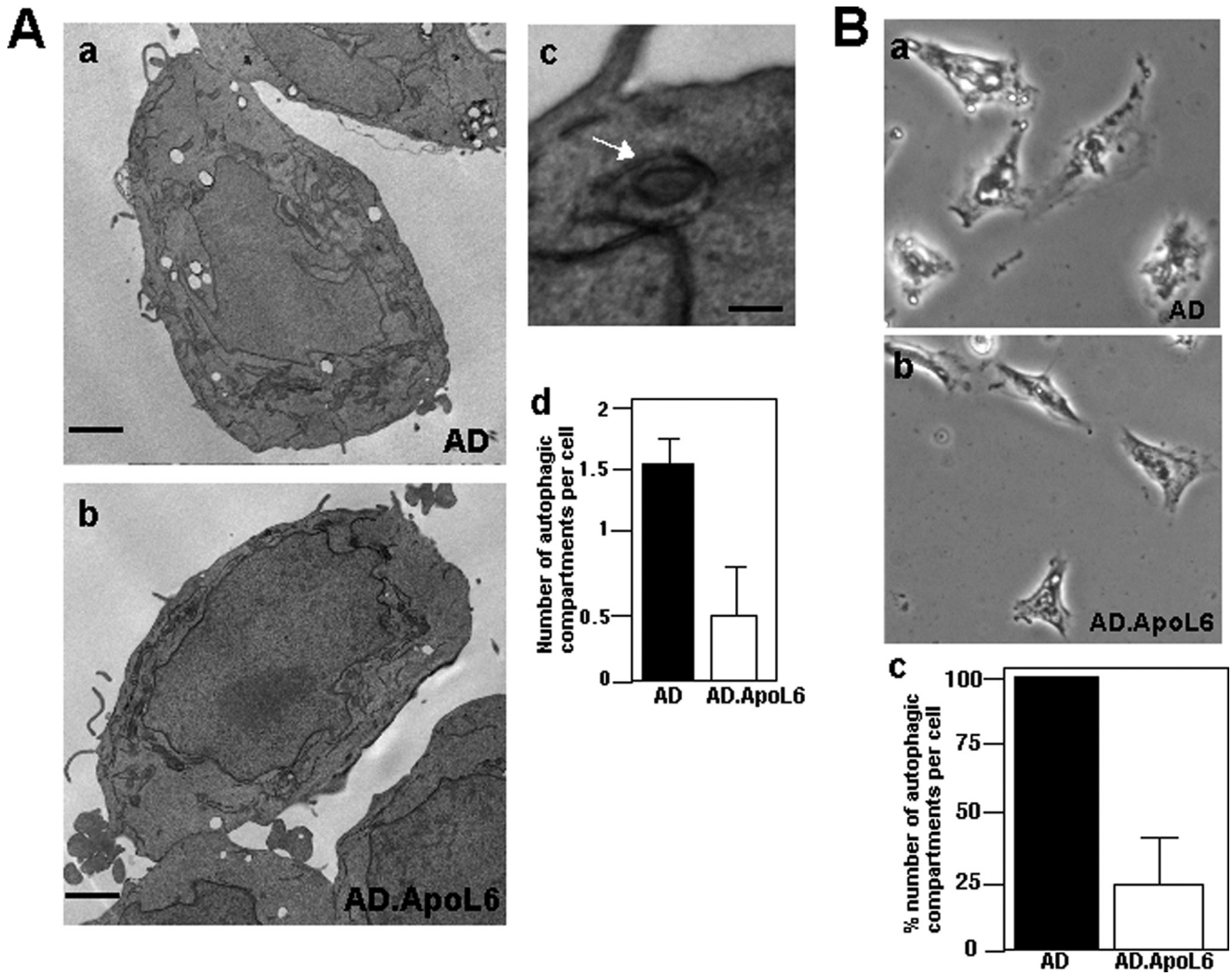

FIGURE 7. **Forced expression of ApoL6 causes autophagy attenuation.** *A*, *TEM analysis* showed that LDCs infected with AD.ApoL6 (*panel b*) for 36 h had significant reduction (to ~30%, *panel d*) in number of autophagic vesicles (AVs)/compartments when compared with LDCs infected with AD only (*panel a*). AVs, defined as double-membrane structures great than 1 μm in size, such as the one marked by *arrow* in *panel c*, were counted and calculated by two independent investigators. At least 200 cells from each group were counted. *B*, MDC staining also showed reduction (to ~25%, *panel c*) of numbers of acidic AVs per cell in LDCs infected with AD.ApoL6 (*panel b*) than in LDCs infected with AD only (*panel a*) (Scale bars: 2 μm (*panels a* and *b*) and 1 μm (*panel c*)). For *B*, the average number of acidic AVs per cell in LDCs infected with AD.ApoL6 was normalized by that of LDCs infected with AD only.

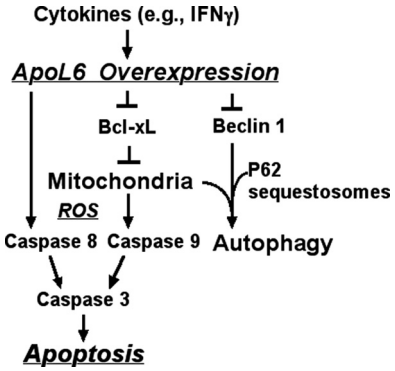

FIGURE 8. **Hypothetical model of ApoL6-induced apoptosis in atherosclerotic lesion cells.** See text for detail.

autophagy can be used to degrade active caspase 8 and therefore blocking apoptosis (55). Our findings demonstrate that ApoL6 is one, if not the major, of the immediate regulators that controls levels and function of Beclin 1, Bcl-X_L, and caspase 8 in apoptosis and autophagy because ApoL6 binds Bcl-X_L, induces Beclin 1 degradation and subsequent autophagy inhibition. Interestingly, one of the functions of autophagy is to degrade damaged, ROS overproducing mitochondria, known as mitophagy. By blocking Beclin 1-dependent autophagy/mitophagy, ApoL6 would cause further accumulation of ROS-producing mitochondria and therefore a positive apoptosis loop (Fig. 8). Thus, the present studies contribute to a better understanding of 1) the role of ApoL6 in the pathobiology of the atherosclerotic plaques; 2) the mechanisms by which ApoL6 may lead to plaque destabilization; and 3) the potential role of small molecules and/or si-ApoL6 as therapeutic agents in atherosclerosis.

REFERENCES

1. Hansson, G. K., and Libby, P. (2006) *Nat. Rev. Immunol.* **6,** 508–519
2. Ross, R. (1993) *Nature* **362,** 801–809
3. Jia, G., Cheng, G., and Agrawal, D. K. (2007) *Autophagy* **3,** 63–64
4. Martinet, W., and De Meyer, G. R. Y. (2009) *Circ. Res.* **104,** 304–317
5. Clarke, M., and Bennett, M. (2006) *Am. J. Nephrol.* **26,** 531–535

6. Hansson, G. K., Robertson, A. K., and Söoderberg-Nauclér, C. (2006) *Annu. Rev. Pathol.* **1,** 297–329
7. Bauriedel, G., Hutter, R., Welsch, U., Bach, R., Sievert, H., and Lüderitz, B. (1999) *Cardiovasc. Res.* **41,** 480–488
8. Geng, Y. J., and Libby, P. (2002) *Arterioscler. Thromb. Vasc. Biol.* **22,** 1370–1380
9. Clarke, M., and Bennett, M. (2006) *Cell Cycle* **5,** 2329–2331
10. Doran, A. C., Meller, N., and McNamara, C. A. (2008) *Arterioscler. Thromb. Vasc. Biol.* **28,** 812–819
11. Kolodgie, F. D., Narula, J., Haider, N., and Virmani, R. (2001) *Cardiol. Clin.* **19,** 127–139, ix
12. Chawla-Sarkar, M., Lindner, D. J., Liu, Y. F., Williams, B. R., Sen, G. C., Silverman, R. H., and Borden, E. C. (2003) *Apoptosis* **8,** 237–249
13. Ravikumar, B., Sarkar, S., Davies, J. E., Futter, M., Garcia-Arencibia, M., Green-Thompson, Z. W., Jimenez-Sanchez, M., Korolchuk, V. I., Lichtenberg, M., Luo, S., Massey, D. C., Menzies, F. M., Moreau, K., Narayanan, U., Renna, M., Siddiqi, F. H., Underwood, B. R., Winslow, A. R., and Rubinsztein, D. C. (2010) *Physiol. Rev.* **90,** 1383–1435
14. Wan, G., Zhaorigetu, S., Liu, Z., Kaini, R., Jiang, Z., and Hu, C. A. (2008) *J. Biol. Chem.* **283,** 21540–21549
15. Pattingre, S., Tassa, A., Qu, X., Garuti, R., Liang, X. H., Mizushima, N., Packer, M., Schneider, M. D., and Levine, B. (2005) *Cell* **122,** 927–939
16. Jia, G., Cheng, G., Gangahar, D. M., and Agrawal, D. K. (2006) *Immunol. Cell Biol.* **84,** 448–454
17. Yan, L., Vatner, D. E., Kim, S. J., Ge, H., Masurekar, M., Massover, W. H., Yang, G., Matsui, Y., Sadoshima, J., and Vatner, S. F. (2005) *Proc. Natl. Acad. Sci. U.S.A.* **102,** 13807–13812
18. Boyle, J. J., Bowyer, D. E., Weissberg, P. L., and Bennett, M. R. (2001) *Arterioscler. Thromb. Vasc. Biol.* **21,** 1402–1407
19. Green, D. R. (1998) *Cell* **94,** 695–698
20. Imanishi, T., Han, D. K., Hofstra, L., Hano, T., Nishio, I., Liles, W. C., Gown, A. M., Schwartz, S. M., and Gorden, A. M. (2002) *Atherosclerosis* **161,** 143–151
21. Kavurma, M. M., Tan, N. Y., and Bennett, M. R. (2008) *Arterioscler. Thromb. Vasc. Biol.* **28,** 1694–1702
22. Seimon, T., and Tabas, I. (2009) *J. Lipid Res.* **50,** (suppl.), S382–S387
23. Schrijvers, D. M., De Meyer, G. R., Kockx, M. M., Herman, A. G., and Martinet, W. (2005) *Arterioscler. Thromb. Vasc. Biol.* **25,** 1256–1261
24. Tabas, I. (2005) *Arterioscler. Thromb. Vasc. Biol.* **25,** 2255–2264
25. Schrijvers, D. M., De Meyer, G. R., Herman, A. G., and Martinet, W. (2007) *Cardiovasc. Res.* **73,** 470–480
26. Chipuk, J. E., Moldoveanu, T., Llambi, F., Parsons, M. J., and Green, D. R. (2010) *Mol. Cell* **37,** 299–310
27. Kutuk, O., and Basaga, H. (2006) *Apoptosis* **11,** 1661–1675
28. Youle, R. J., and Strasser, A. (2008) *Nat. Rev. Mol. Cell Biol.* **9,** 47–59
29. Pollman, M. J., Hall, J. L., Mann, M. J., Zhang, L., and Gibbons, G. H. (1998) *Nat. Med.* **4,** 222–227
30. Saxena, A., McMeekin, J. D., and Thomson, D. J. (2002) *J. Pathol.* **196,** 335–342
31. Gagarin, D., Yang, Z., Butler, J., Wimmer, M., Du, B., Cahan, P., and McCaffrey, T. A. (2005) *J. Mol. Cell Cardiol.* **39,** 453–465
32. Yang, Z., Gagarin, D., Ramezani, A., Hawley, R. G., and McCaffrey, T. A. (2007) *J. Vasc. Res.* **44,** 483–494
33. Lomonosova, E., and Chinnadurai, G. (2008) *Oncogene* **27,** Suppl. 1, S2–S19
34. Yang, Z., Gagarin, D., St Laurent, G., 3rd, Hammell, N., Toma, I., Hu, C. A., Iwasa, A., and McCaffrey, T. A. (2009) *Arterioscler. Thromb. Vasc. Biol.* **29,** 1213–1219
35. Du, B., Fu, C., Kent, K. C., Bush, H., Jr., Schulick, A. H., Kreiger, K., Collins, T., and McCaffrey, T. A. (2000) *J. Biol. Chem.* **275,** 39039–39047
36. McCaffrey, T. A., Fu, C., Du, B., Eksinar, S., Kent, K. C., Bush, H., Jr., Kreiger, K., Rosengart, T., Cybulsky, M. I., Silverman, E. S., and Collins, T. (2000) *J. Clin. Invest.* **105,** 653–662
37. Liu, Z., Lu, H., Jiang, Z., Pastuszyn, A., and Hu, C. A. (2005) *Mol. Cancer Res.* **3,** 21–31
38. Liu, Z., Lu, H., Shi, H., Du, Y., Yu, J., Gu, S., Chen, X., Liu, K. J., and Hu, C. A. (2005) *Cancer Res.* **65,** 1647–1654
39. Pankiv, S., Clausen, T. H., Lamark, T., Brech, A., Bruun, J. A., Outzen, H., Øvervatn, A., Bjørkøy, G., and Johansen, T. (2007) *J. Biol. Chem.* **282,** 24131–24145
40. Donald, S. P., Sun, X. Y., Hu, C. A., Yu, J., Mei, J. M., Valle, D., and Phang, J. M. (2001) *Cancer Res.* **61,** 1810–1815
41. Köchl, R., Hu, X. W., Chan, E. Y., and Tooze, S. A. (2006) *Traffic* **7,** 129–145
42. Sun, Q., Fan, W., Chen, K., Ding, X., Chen, S., and Zhong, Q. (2008) *Proc. Natl. Acad. Sci. U.S.A.* **105,** 19211–19216
43. Kang, R., Zeh, H. J., Lotze, M. Y., and Tang, D. (2011) *Cell Death Diff.* **18,** 571–580
44. Mizushima, N., Yoshimori, T., and Levine, B. (2010) *Cell* **140,** 313–326
45. Komatsu, M., Waguri, S., Koike, M., Sou, Y. S., Ueno, T., Hara, T., Mizushima, N., Iwata, J., Ezaki, J., Murata, S., Hamazaki, J., Nishito, Y., Iemura, S., Natsume, T., Yanagawa, T., Uwayama, J., Warabi, E., Yoshida, H., Ishii, T., Kobayashi, A., Yamamoto, M., Yue, Z., Uchiyama, Y., Kominami, E., and Tanaka, K. (2007) *Cell* **131,** 1149–1163
46. Bjørkøy, G., Lamark, T., Brech, A., Outzen, H., Perander, M., Overvatn, A., Stenmark, H., and Johansen, T. (2005) *J. Cell Biol.* **171,** 603–614
47. Niemann, A., Baltes, J., and Elsässer, H. P. (2001) *J. Histochem. Cytochem.* **49,** 177–185
48. Hayakawa, Y., Takemura, G., Misao, J., Kanoh, M., Ohno, M., Ohashi, H., Takatsu, H., Ito, H., Fukuda, K., Fujiwara, T., Minatoguchi, S., and Fujiwara, H. (1999) *Arterioscler. Thromb. Vasc. Biol.* **19,** 2066–2077
49. Kim, P. K., Hailey, D. W., Mullen, R. T., and Lippincott-Schwartz, J. (2008) *Proc. Natl. Acad. Sci. U.S.A.* **105,** 20567–20574
50. Komatsu, M., and Ichimura, Y. (2010) *FEBS Lett.* **584,** 1374–1378
51. Rosner, D., Stoneman, V., Littlewood, T., McCarthy, N., Figg, N., Wang, Y., Tellides, G., and Bennett, M. (2006) *Am. J. Pathol.* **168,** 2054–2063
52. Chan, S. W., Hegyi, L., Scott, S., Cary, N. R., Weissberg, P. L., and Bennett, M. R. (2000) *Circ. Res.* **86,** 1038–1046
53. Cho, D. H., Jo, Y. K., Hwang, J. J., Lee, Y. M., Roh, S. A., and Kim, J. C. (2009) *Cancer Lett.* **274,** 95–100
54. Luo, S., and Rubinsztein, D. C. (2010) *Cell Death Differ.* **17,** 268–277
55. Hou, W., Han, J., Lu, C., Goldstein, L. A., and Rabinowich, H. (2010) *Autophagy* **6,** 891–900